A Versatile Workflow of Pore Geometry-Structure Rock Typing and Corey Parameter-Based Relative Permeability Trend Modeling

Muhammad Nur Ali Akbar[1], *Ardian* Pradhana Putra[2] and *Matthew* Guy Reppert[2]

[1]Prores AS, Subsurface – Sendra, 7041 Trondheim, Norway
[2]Vår Energi, Subsurface, 4313 Sandnes, Norway

Abstract. This study introduces an integrated method for incorporating flow properties from special core analysis (SCAL) experiments into rock type definitions for comprehensive reservoir characterization. The method involves generating rock types based on pore geometry-structure (PGS) similarity using porosity and permeability data. Flow properties from SCAL simulations are parameterized to analyze endpoint saturations and Corey curve shapes for each SCAL experiment. These parameters are stored in a SCAL database and analyzed against initial water saturation, porosity, and permeability. A case study from the Norwegian Continental Shelf demonstrates this approach, resulting in the establishment of 11 rock types based on PGS rock type curves, later generalized into 6 groups. Each rock type is equipped with representative saturation functions, including base-case, optimistic, and pessimistic bounds. Aggregated SCAL experiments develop representative saturation functions consistent with wettability and rock properties for full-field application. This method enables the parameterization, utilization of trend models, and identification of analogs from the database, resulting in well-defined saturation functions. The resulting relative permeability and rock types are suitable for full-field reservoir simulations, uncertainty analyses, and field performance assessments.

1 Introduction

Rock typing plays a crucial role in reservoir characterization, particularly in enhancing the evaluation of complex reservoir rock properties such as permeability prediction, distribution of static water saturation based on saturation height models, and characterization of dynamic flow behavior based on relative permeability. Various rock typing methods have been developed and widely implemented in numerous case studies, encompassing sandstone [1], carbonate [2], and other intricate reservoir rocks like naturally fractured basement [3] and unconventional organic-rich shale [4].

Currently, the oil and gas industry extensively employs a multitude of rock typing methodologies, drawing from geological, engineering, rock physics, and geostatistical approaches across different scales. These methods range from simple empirical approaches [5-8], utilizing permeability, porosity, and irreducible water saturation data, to more complex hydraulic flow unit methods [9, 10, 11]. Some methodologies also incorporate capillary pressure data and the J-function [12, 13, 14], and radius r35 measurements [15, 16]. Geological descriptions based on petrographic data, including rock fabric, depositional environment, texture, and depositional facies, are also commonly considered [17, 18, 19]. Additionally, geostatistical techniques such as clustering [20], self-organizing maps [21], and fuzzy logic [22] are frequently utilized.

In terms of relative permeability trend modeling, Ebeltoft et al. [23] introduced a method utilizing LET relative permeability parameters developed by Lomeland et al. [24]. This approach aims to ensure wettability-consistent flow properties, capture uncertainty in relative permeability for full-field applications and generate synthetic relative permeability data from analog special core analysis (SCAL) databases.

This paper proposes a versatile workflow integrating reservoir rock typing based on pore geometry-structure (PGS) rock typing methods and newly developed Corey flow parameters-based trend modeling. This integrated approach aims to enhance reserves assessment during reservoir simulation and field development panning of a recent oil and gas discovery on the Norwegian Continental Shelf (NCS).

2 Study Workflow

Based on Figure 1, we commenced the study workflow by thoroughly quality checking the core data (RCA and SCAL) along with other pertinent information to ensure the accuracy and appropriateness of all data utilized in this study. Subsequently, we applied the PGS method for rock typing, incorporating RCA and SCAL data, and

*Corresponding author: Muhammad.aliakbar@prores.no

seamlessly integrated them into Corey trend modeling to establish rock physics functions for each rock type, facilitating both static and dynamic reservoir modeling. Following this, we estimated the SCAL uncertainty range for each rock type and integrated it into the 3D dynamic model.

Once all input data were assimilated into the reservoir models, we conducted production forecasts using sensitivity and uncertainty workflows to evaluate the better uncertainty of the reserve evaluation of this Field X discovery.

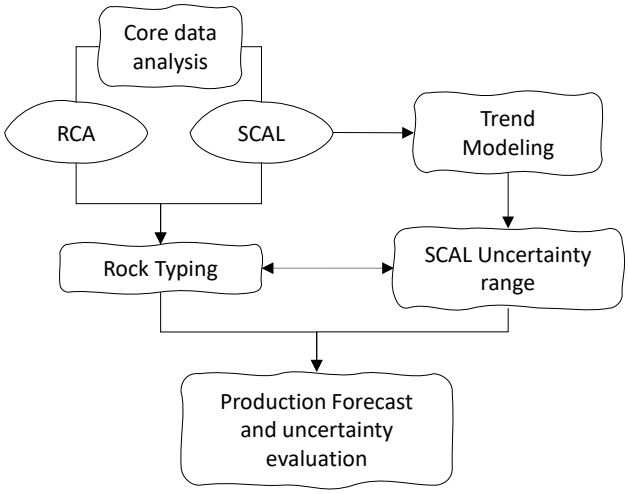

Fig. 1. Study workflow of this study.

3 Data Used

The data used in this study were derived from an oil and gas discovery case on the Norwegian Continental Shelf (NCS) with a focus on core analyses and 3D dynamic modeling.

We began by conducting a quality check of the Routine Core Analysis (RCA) data and then analyzed the interpreted SCAL results from the Sendra Cloud Core Flood Simulator. One example of the relative permeability correction through coreflood simulation is presented in Figure **A-1** in the appendix page. Out of 1,477 core samples from the RCA data, we utilized 1,242 samples, incorporating eight samples in a clean state and 13 in a restored state from the SCAL analyses, which included capillary pressure and relative permeability. Some data were excluded from the evaluation due to reasons such as non-representative data, excessively low porosity and permeability, unreliable measurements, amorphous samples, and experimental errors.

4 Pore Geometry-Structure Rock Typing

This investigation employs the concept of pore geometry-structure rock typing. Rock samples are classified following the rock type curve proposed by Wibowo and Permadi [25], which relies on the similarity of the Kozeny constant [26]. This constant is derived from the product of the pore shape factor (F_s) and tortuosity (τ). The specific internal surface area (S_b) serves as a parametric variable for each rock group. This method of rock grouping facilitates the examination of key factors systematically influencing the capillary pressure [27, 28, 29] and relative permeability groups [30] especially irreducible water saturation. The rearranged Kozeny equation in PGS rock typing can be expressed in two forms:

$$\left(\frac{k}{\phi}\right)^{0.5} = \phi\left(\frac{1}{(\tau F_s {S_b}^2)}\right)^{0.5}, \quad (1)$$

and

$$\frac{k}{\phi^3} = \frac{1}{\tau F_s {S_b}^2}, \quad (2)$$

Here, k represents permeability and ϕ denotes porosity. The term $(k/\phi)^{0.5}$ characterizes pore geometry, often referred to as the "mean hydraulic radius", while (k/ϕ^3) is termed the "pore structure", encompassing all aspects of the internal structure of pore spaces. The additional parameters τ, F_S, and S_b represent tortuosity, pore shape factor, and specific internal surface area, respectively. Equation 1 can be reformulated as a power-law equation for rock typing:

$$\left(\frac{k}{\phi}\right)^{0.5} = a\left(\frac{k}{\phi^3}\right)^{b}. \quad (3)$$

Plotting $(k/\phi)^{0.5}$ against (k/ϕ^3) on a logarithmic scale results in a straight line with a constant a=1 and a maximum exponent slope b=0.5 for perfectly rounded pore shapes and smooth capillary tubes. For natural porous rocks, the value of b must be less than 0.5. The lower the b value, the more complex the pore system of the rock. The constant a serves as a correction factor for volumetric fluid flow efficiency in irregular pore systems [25, 27].

As illustrated in Figure 2(a), eleven rock types (RT-4 to RT-15) were identified using the PGS type curve, where the rock samples align. However, for simplification, we categorized the rock types into six groups and assigned them new names as follows:

- Group 1: Samples falling on the RT-4 line.
- Group 2: Samples falling on the RT-5 line.
- Group 3: Samples falling on the RT-6 line.
- Group 4: Samples falling on the RT-7 line.
- Group 5: Samples falling on the RT-8 line.
- Group 6: Combination samples falling between RT-9 and RT-15 lines.

If we translate this PGS plot into porosity vs. permeability, the grouping results can be seen in Figure 2(b). The border in each rock type was determined based on the study of Wibowo [27].

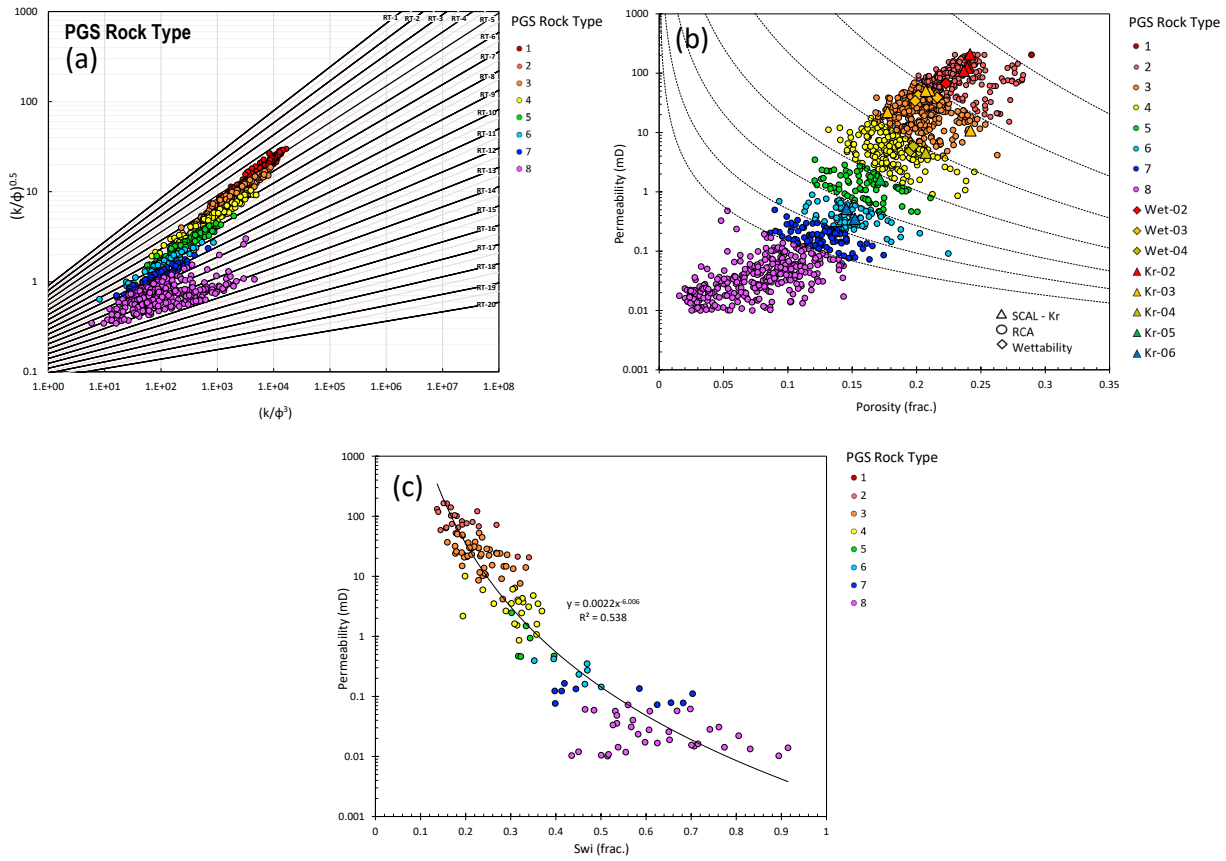

Fig. 2. (a) Rock typing results based on PGS rock type curves; (b) porosity-permeability cross plot with the PGS rock typing results. (c) permeability-initial water saturation cross plot grouped by PGS rock typing results.

Moreover, the initial water saturation (*Swi*) from Dean-Stark (DS) analysis exhibits a good correlation against absolute permeability with distinguishable group in each rock type based on the PGS method.

Subsequently, the resulting rock types were spatially distributed within the existing 3D static model. The study utilized static and dynamic 3D models comprising approximately 3.8 million grid cells, delineating eight reservoir regions. Each grid cell has a lateral resolution of 50m x 50m and a vertical resolution of 1m. The distribution of rock types within these models was determined based on existing 3D petrophysical properties (Figure 3), including porosity, permeability, net-to-gross (NTG) ratio, and static water saturation. The vertical distribution of rock types in well sections and their lateral distribution in 3D space can be observed in Figures 3 and 4, respectively.

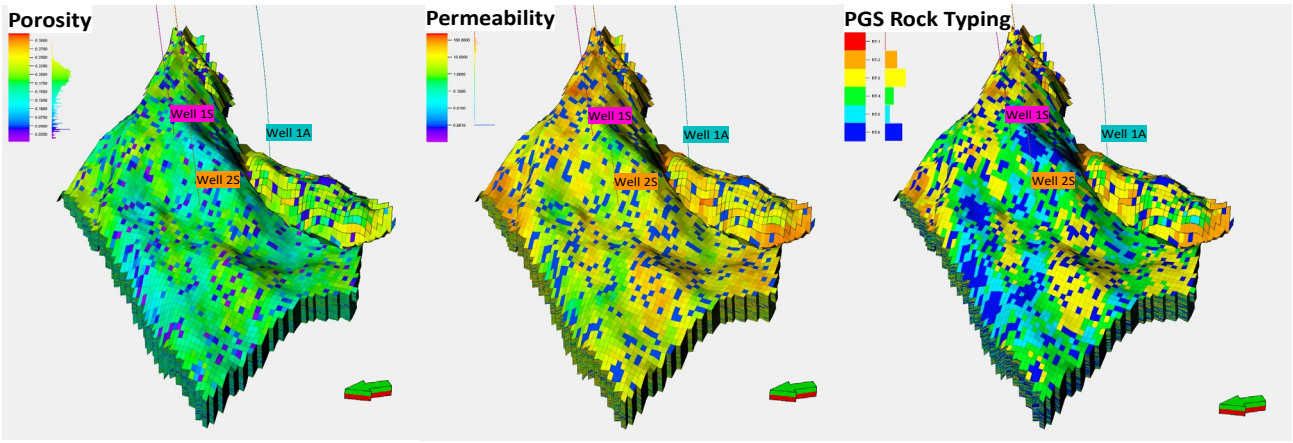

Fig. 3. Porosity, Permeability, and PGS rock type distributions in 3D model.

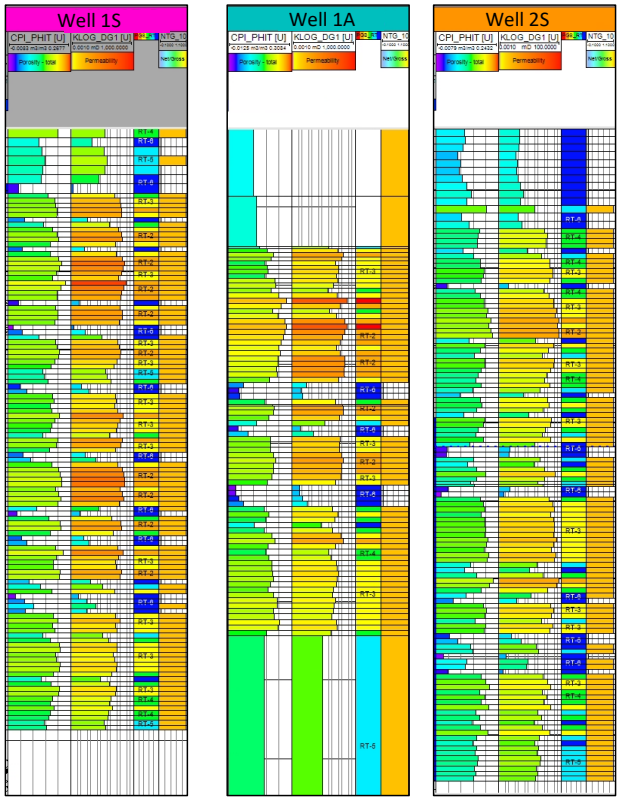

Fig. 4. Porosity, Permeability, and PGS rock type distributions in well section.

5 Corey Trend Modelling

SCAL trend modeling is an automated and comprehensive workflow designed to derive representative saturation functions suitable for full-field applications [23, 31]. This process involves parameterizing flow properties to analyze endpoint saturations and curve shapes for each SCAL experiment individually. The resulting parameters are stored in a SCAL database along with plug data, experimental conditions, and geo-references such as well name, plug depth, and fluid viscosities at reservoir conditions. Multiple parameterized SCAL experiments are then combined to generate representative saturation functions for full-field applications, ensuring consistency with wettability and rock properties. The development of SCAL modeling is grounded in the underlying theory of wettability, reservoir physics, and the observed behavior of a substantial dataset from the Norwegian Continental Shelf.

Corey trend modeling is a novel development in this study, adopting the concept upon previous work by Ebeltoft et al. [23]. The Corey relative permeability is formulated as follows:

$$k_{ro} = k_{ro}^{0}(1 - S_w^*)^{no} \tag{4}$$

$$k_{rw} = k_{rw}^{0}(S_w^*)^{nw} \tag{5}$$

$$S_w^* = \frac{S_w - S_{wir}}{1 - S_{orw} - S_{wir}} \tag{6}$$

k_{ro}^{0} is the end point relative permeability to oil at irreducible water saturation (S_{wir}) and k_{rw}^{0} is the end point relative permeability to water at residual oil saturation (S_{orw}). Meanwhile *no* and *nw* are the curve shape of Corey exponent for oil and water, respectively.

In Corey correlation, each flow parameter is linked to individual trend models, determined as functions of S_{wi}. These models, grounded in physics and wettability principles, are calibrated using a SCAL database. Designed to replicate the typical scatter observed in experimental data, these trend models yield relative permeability curves while adhering to wettability and physical characteristics governing multi-phase flow in porous media. Each model is meticulously calibrated to match the field-specific SCAL data, with a focus on water-oil imbibition.

The formulation of the trend modeling is a simplification from the previous study by Ebeltoft et al. [23], maintaining identical trend behavior of initial water saturation against residual oil saturation, end-point relative permeability to water, and Corey exponents of oil and water. Modified from Lomeland et al. [31], we have derived the correlation between S_{wi} and S_{orw} [31] as follows:

$$S_{orw} = C_{S_{orw}} + \left(A_{S_{orw}} - C_{S_{orw}} + B_{S_{orw}} \times S_{wi}^{M_{S_{orw}}}\right) \times (1 - S_{wi})^{O_{S_{orw}}} \tag{7}$$

The typical trend for this relationship is shown in Figure 5(a) and coincides with the wettability study by Spiteri et al. [32]. The trend is consistent with increasing S_{orw} by increasing S_{wi} until a maximum is reached where S_{orw} decreases with increasing S_{wi}.

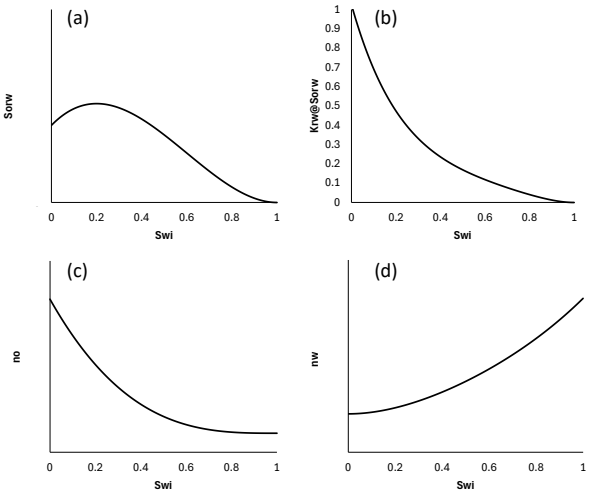

Fig. 5. Typical trend models for (a) *Sorw* vs. *Swi* by use of Equation 7; (b) end-point relative permeability to water as a function of *Swi* by use of Equation 8; (c) Corey exponent of oil, *no* vs. *Swi;* (d) Corey exponent of water, *nw* vs. *Swi*.

Relative permeability and wettability are known to be correlative [33]. Enhanced water-wettability typically leads to lower endpoint relative permeability to water [34] and a broader suppression of relative permeability to water across the entire mobile saturation range. This relationship between S_{wi} and wettability forms the foundation for the trend model connecting endpoint water relative permeability to S_{wi}, as developed by Lomeland et al [23, 31] and represented by Equation 8. However, in this context, the model is further refined with the inclusion of maximum parameter A_{Krw} and minimum parameter C_{Krw} to enhance its general applicability.

$$K_{rw} = C_{K_{rw}} + \left(\left(A_{K_{rw}} - C_{K_{rw}} \right) \times (1 - S_{orw} - S_{wi})^{Ok_{rw}} \right) \quad (8)$$

The typical trend model illustrating the relationship between end-point relative permeability to water ($k_{rw}(S_{orw})$) and S_{wi} is depicted in Figure 5(b). This model aligns with the understanding that an increase in S_{wi} correlates with heightened water-wettability, resulting in decreased relative permeability to water. The trend model for $k_{rw}(S_{orw})$ is intricately linked to the trend model for S_{orw} versus S_{wi} presented in Figure 5(a). A low S_{wi} corresponds to a low S_{orw}, thereby yielding a high $k_{rw}(S_{orw})$. Conversely, while a high S_{wi} also corresponds to a low S_{orw}, it also signifies significantly water-wet conditions, leading to a lower $k_{rw}(S_{orw})$.

The shapes of the relative permeability curves are delineated by Corey parameters for oil and water. It's crucial that the trend models for these parameters accurately reflect the changes in wetting behavior as S_{wi} varies. Figure 5(c) illustrates typical trend models for Corey shape parameters for oil. As S_{wi} increases, the system becomes more water-wet, leading to higher oil relative permeability, consistent with the trend models displayed. Similarly, trend models for Corey parameters for water are depicted in Figure 5(d). These models align with the notion that increasing S_{wi} induces a more water-wet system, resulting in lower relative permeability and a more depressed shape of the water curve. Conversely, a shift towards more oil-wet behavior corresponds to higher water relative permeability.

6 Field-Specific Trend Models

Wettability and relative permeability are influenced not only by S_{wi} but also by the chemical interactions among crude oil, brine, and rock (COBR) [34-40], as well as by geological characteristics such as mineralogy, clay content, and pore size distribution. Therefore, it is crucial to refine the trend model to integrate insights from special core analysis measurements specific to the field under study. This process involves interpreting relevant SCAL experiments and parameterizing all relative permeabilities according to the Corey formulation. These parameters, along with plug data and geo-references (well name, depth, formation name, etc.), are stored in a SCAL database, enabling the calibration of individual trend models to the field-specific properties.

The calibrated trend models, depicted in Figure 6, incorporate orange points representing plug measurements from oil discovery X. Three models are introduced, including a base model bounded by high and low models, effectively capturing the scatter present in the SCAL data and providing a field-specific trend model for S_{orw} versus S_{wi}, along with a range of uncertainty. Calibration, conducted via visual inspection guided by the described trend models and field-specific SCAL data, offers several advantages, including easy identification of outliers, straightforward evaluation of data scatter, and rapid calibration of trend models to encompass base-case trends along with high and low bounds for uncertainty.

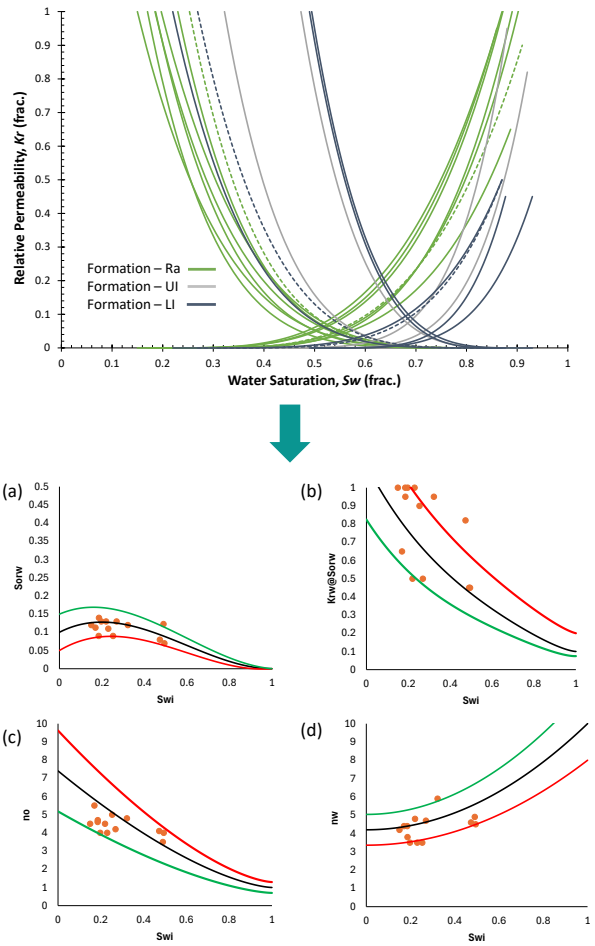

Fig. 6. Relative permeability data (upper figure) and trend modelling of a specific oil discovery from the NCS from Formations of Ra, UI and LI. Black lines in trend modelling exhibit the expected model, bounded by high and low trends in green and red to capture uncertainty. (a) *Sorw* vs. *Swi*; (b) end-point relative permeability to water as function of *Swi*; (c) Corey exponent of oil, *no* vs. *Swi;* (d) Corey exponent of water, *nw* vs. *Swi*.

Once all Corey parameters are calibrated, full-field relative permeability curves are generated using field-specific trend models incorporating defined PGS rock

types. A summary of parameterized relative permeability and averaged S_{wi} in each rock type, along with its uncertainty span, is presented in Table 1.

Table 1. Parameterized SCAL Summary for each PGS rock type

		PGS Rock Type					
	Parameters	1	2	3	4	5	6
Base	Swi	0.2	0.23	0.28	0.36	0.45	0.63
	Krw@Sorw	0.76	0.72	0.66	0.57	0.48	0.24
	no	5.58	5.32	4.91	4.28	3.61	2.44
	nw	4.43	4.51	4.65	4.95	5.37	6.50
	Sorw	0.23	0.23	0.22	0.21	0.19	0.13
Opt.	Swi	0.2	0.23	0.28	0.36	0.45	0.63
	Krw@Sorw_low	0.54	0.51	0.46	0.39	0.33	0.22
	no_low	3.91	3.73	3.44	2.99	2.53	1.71
	nw_high	5.32	5.41	5.59	5.94	6.45	7.80
	Sorw_high	0.17	0.17	0.16	0.15	0.13	0.08
Pess.	Swi	0.20	0.23	0.28	0.36	0.45	0.63
	Krw@Sorw_high	1.00	0.97	0.90	0.78	0.67	0.48
	no_high	7.25	6.92	6.38	5.56	4.69	3.17
	nw_low	3.55	3.61	3.72	3.96	4.30	5.20
	Sorw_low	0.09	0.09	0.09	0.08	0.07	0.04

Throughout this paper, S_{wi} refers to saturation established at high capillary pressure using a porous plate or centrifuge around 12.6 bar, including S_{wi} measured from Dean-Stark, closely resembling irreducible water saturation (S_{wir}). Consequently, emphasis is placed on the reservoir region above the capillary transition zone, where production wells initiate oil production without water content. S_{wir} varies with absolute permeability across the reservoir, defining the lowest water saturation and anchoring the relative permeability curves.

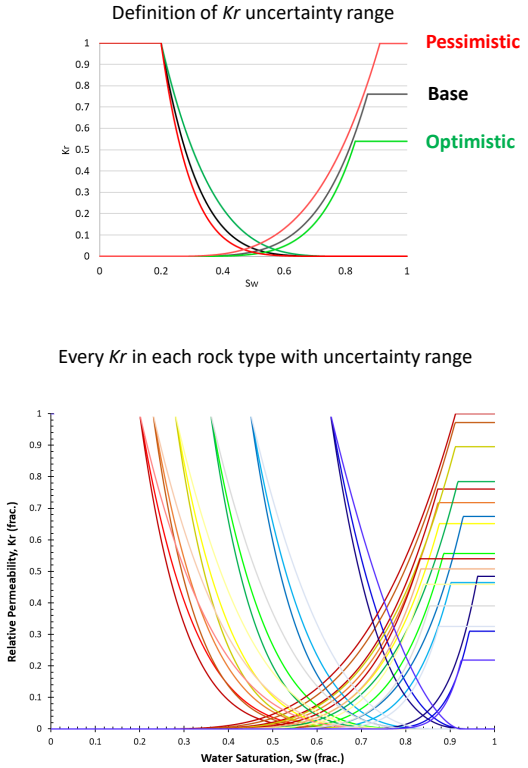

Fig. 7. Relative permeability curves generated from Corey trend modelling with uncertainty span in each rock group.

Figure 7 (upper) illustrates the resulting relative permeability curves for PGS rock group 1 with S_{wi} = 0.2, encompassing *base*, *optimistic*, and *pessimistic* scenarios. Figure 7 (lower) shows the resulting base case relative permeabilities for all six rock groups, with S_{wi} for each rock group presented in Table 1. It is important to note that both the shape and endpoints of the relative permeability curves change as S_{wi} increases in each rock group. To compare the estimated relative permeability results from Corey trend modeling and PGS rock typing against the original experiment data, Figure A-2 in the appendix presents this comparison.

7 Reservoir Simulation Study

The study's investigation into relative permeability uncertainty significantly impacts the assessment of recoverable reserves in 3D reservoir simulation. In term of recoverable volume estimation, we represent the calculation based on the oil recovery factor (RF) calculation. The oil recovery factor is a crucial parameter in petroleum engineering, representing the fraction of the total oil in place (OOIP) that can be economically recovered from a reservoir. The recovery factor is calculated using the following formula:

$$RF = \frac{Cumulative\ Oil\ Production}{OOIP} \times 100\%, \quad (9)$$

where, Cumulative Oil Production is the total amount of oil produced from the reservoir up to a given time.

Due to the confidentiality of the data, we cannot present the exact volume of the production forecast of this simulation study. However, considering the equation 9 for calculating the RF with all possible relative permeability data from the case study, the estimated recovery factor exhibits an uncertainty range from 29% to 45%, as depicted in Figure 8 alongside typical oil production, reservoir pressure, and water injection profiles.

Through the implementation of the newly developed Corey trend modeling approach, incorporating the defined uncertainty span illustrated in Figure 7, we can narrow the uncertainty span of the oil recovery factor to a range of 34% - 41%, as shown in Figure 9. This represents a significant reduction from the initial uncertainty span of 16%, down to 7%. Consequently, this refinement enhances the value of SCAL uncertainty studies, particularly in 3D dynamic reservoir simulation, facilitating improved decision-making regarding the evaluation of recoverable reserves for specific assets in exploration or early development phases.

Furthermore, this method is expected to enhance the quality of full static and dynamic modeling workflows, particularly in advancing history matching and production forecasting in developing fields, both in the short and long term. Ultimately, this workflow fosters a deeper understanding of consistent physical models and wettability concepts.

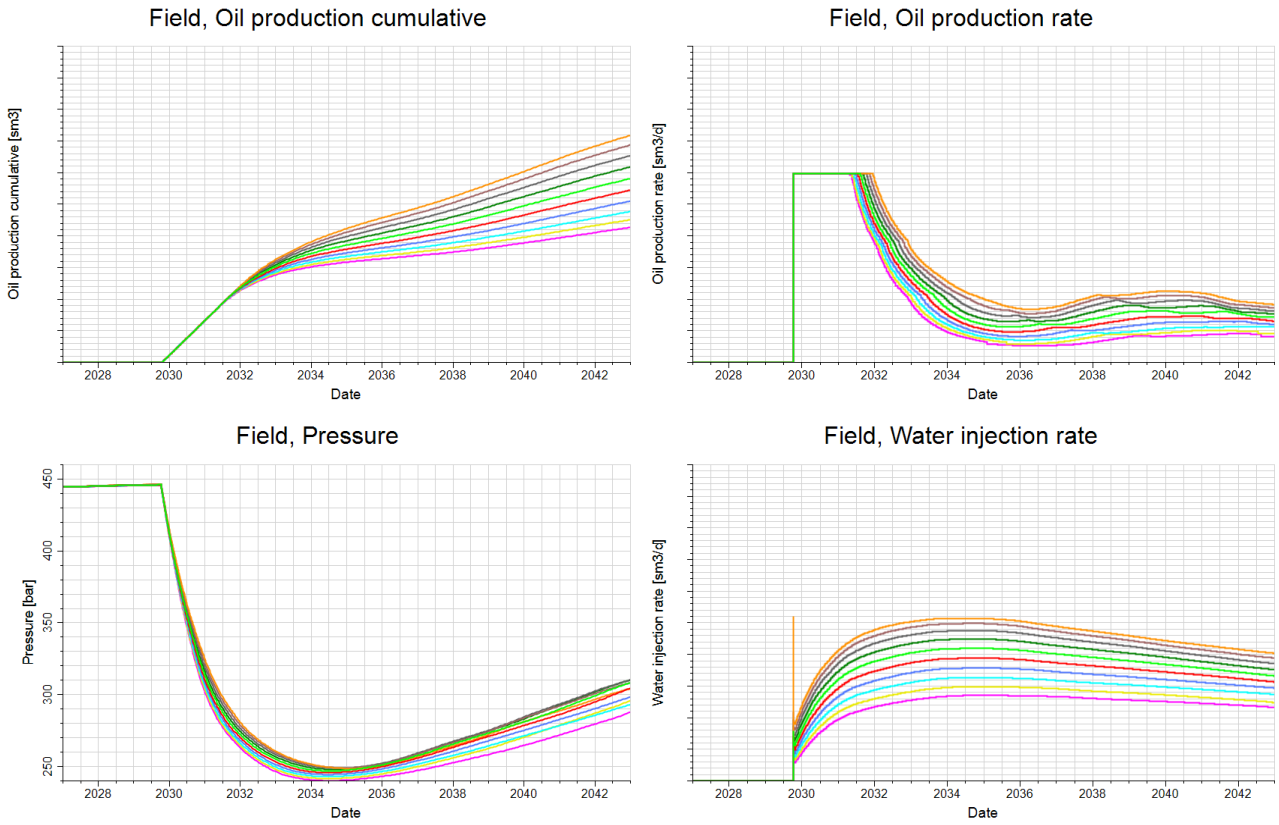

Fig. 8. Production forecast profile in Field X showcasing relative permeability sensitivity and uncertainty data.

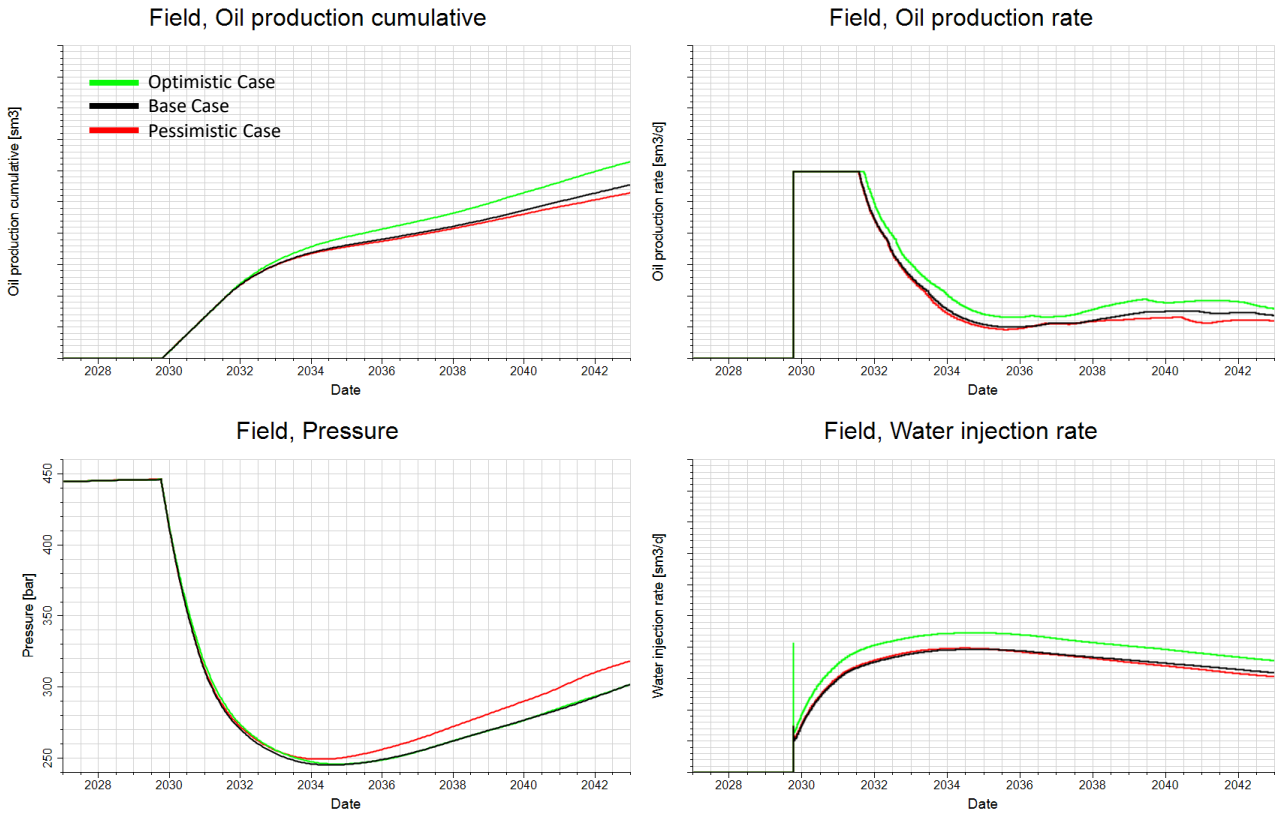

Fig. 9. Production forecast profile in oil discovery X displaying the uncertainty span derived from the new Corey trend modelling method.

8 Conclusions

The conclusions of this paper can be summarized as follows:

- This paper merged the methodology of PGS rock typing (Wibowo et al, 2013) and parameter based SCAL (Ebeltoft et al , 2014).
- Integrating the PGS rock typing and newly developed Corey trend modelling provide a versatile workflow to evaluate the relative permeability uncertainty for full-field applications.
- Parameterizing Corey flow properties streamlines the utilization of extensive SCAL datasets for defining static and dynamic saturation functions for reservoir modeling, enhancing the efficiency and capture better uncertainty of reservoir characterization for full-field applications.
- By incorporating PGS rock typing, wettability concept, and the physics of flow in porous media, trend models are developed to accurately represent end points and shape parameters of relative permeability, ensuring consistency with fluid flow behavior in reservoir/ porous medium.
- Acknowledging the inherent scatter in SCAL data, the Corey developed trend models provide guidance for constructing smooth curves suitable for full-field simulation, enhancing the reliability of reservoir models.
- The generation of SCAL models/saturation functions with base, optimistic, and pessimistic bounds allows for thorough evaluation and uncertainty analysis of recoverable reserves, providing valuable insights for specific fields and aiding decision-making processes.

Acknowledgement

The authors would like to acknowledge Vår Energi ASA for granting permission to publish the data and the full paper.

References

1. A.M.A. El-Sayed, Sayed, N.A.E., Ali, H.A. et al. *Rock typing based on hydraulic and electric flow units for reservoir characterization of Nubia Sandstone, southwest Sinai, Egypt*. Journal of Petrol Explor Prod Technol 11, 3225–3237 (2021).
2. R. Mohebian, Riahi, M.A. & Kadkhodaie, *A. Characterization of hydraulic flow units from seismic attributes and well data based on a new fuzzy procedure using ANFIS and FCM algorithms, example from an Iranian carbonate reservoir*. Journal of Carbonates Evaporites 34, 349–358 (2019).
3. M.N. Ali Akbar, *Naturally Fractured Basement Reservoir Characterization in a Mature Field.* In SPE *Annual Technical Conference and Exhibition*, Dubai, UAE. DOI: 10.2118/206027-MS , (2021).
4. M.N. Ali Akbar and J.T. Musu, *An Extensive Petrophysical Evaluation for Determining Sweet Spot Intervals in the Ultra-Tight Organic-Rich Shale: A Case Study of the North Sumatra Basin,* in *SPWLA 2nd Asia Pacific Technical Symposium*, Bogor, Java, Indonesia, (2018).
5. G.E. Archie, Introduction to Petrophysics of Reservoir Rocks, Bulletin of the American Association of Petroleum Geologists, vol. 34, no. 5, 943 – 961. (1950).
6. G.E. Archie, *Classification of Carbonate Reservoir Rocks and Petrophysical Consideration*, Bulletin of the American Association of Petroleum Geologists, vol. 36, no. 2, 278 – 298. (1952).
7. S. Kolodzie, *Analysis of pore throat size and use of the Waxman-Smits equation to determine OOIP in Spindle field, Colorado*. SPE-9382-MS. In SPE *Annual Technical Conference and Exhibition*, Dallas, Texas (1980).
8. E.D. Pittman, *Relationship of Porosity and Permeability to Various Parameters Derived from Mercury Injection – Capillary Pressure Curves for Sandstone*, Bulletin Of The American Association Of Petroleum Geologists, vol. 76, no. 2, 191 – 198 (1992).
9. J.O. Amaefule, Altunbay, M., Tiab, D., Kersey, D.G., Keelan, D.K. *Enhanced reservoir description using core and log data to identify hydraulic flow units and predict permeability in uncored intervals/wells.* In SPE *Annual Technical Conference and Exhibition*, Houston, Texas (1993).
10. P.W.M. Corbett, and Potter, D.K., *Petrotyping: A Basemap and Atlas for Navigating Through Permeability and Porosity Data for Reservoir Comparison and Permeability Prediction,* In International Symposium of *the Society of Core Analysts*, Abu Dhabi, UAE, (2004).
11. Abbaszadeh, M., Fujii, H., Fujimoto, F. (1996). Permeability prediction by hydraulic flow units - theory and applications. SPE Form. Eval. 11, 263–271.
12. Leverett, M.C. (1940). Capillary Behavior in Porous Solids, Petroleum Technology, 1223, 152– 169. El-Khatib, (1995).
13. El-Khatib, N. Development of a Modified Capillary Pressure J-Function, Paper SPE 29890 presented at the SPE Middle East Oil Show held in Bahrain, March 11-14, (1995).
14. Xu, C., Torres-Verdín, C., (2013). Pore system characterization and petrophysical rock

classification using a bimodal Gaussian density function. Math. Geosci.Kolodzie, (1980).

15. A.J. Martin, Stephen T. Solomon, Dan J. Hartmann; *Characterization of Petrophysical Flow Units in Carbonate Reservoirs*. AAPG Bulletin 81 (5): 734–759, (1997).
16. Gunter, G.W., Finneran, J.M., Hartman, D.J. dan Miller, J.D. Early Determination of Reservoir Flow Units Using an Integrated Petrophysical Method, Paper SPE 38679 presented at SPE Annual Technical Conference and Exhibition held in San Antonio, Texas, October 5 – 8, (1997).
17. Jenings Jr., and Lucia, J.F., Predicting Permeability From Well Logs in Carbonates With a Link to Geology for Interwell Permeability Mapping, SPE Formation Evaluation and Engineering, (2003).
18. Dunham, R.J., Classification Of Carbonate Rocks According To Depositional Texture, Memoir of the American Association of Petroleum Geologists, 1, 108 – 121, (1962).
19. Skalinski, M., Zeh, S.G., dan Moss, B., Defining and Predicting Rock Types in Carbonates – Preliminary Results from an Integrated Approach Using Core and Log Data in Tengiz Field, SPWLA 46th Annual Logging Symposium, June 26 – 29, (2005).
20. Akbar, M., Szabo, N.P. and Dobróka, M., An Automated and Robust Solution of K-Means Cluster Analysis Based on Most Frequent Value Approach. In 82nd EAGE Annual Conference & Exhibition (Vol. 2021, No. 1, pp. 1-5). European Association of Geoscientists & Engineers. (2021).
21. Akbar, Muhammad Nur Ali & Nemes, István & Bihari, Zsolt & Soltész, Helga & Bárány, Ágnes & Tóth, László & Borka, Szabolcs & Ferincz, György. Naturally Fractured Carbonate Reservoir Characterization: A Case Study of A Mature High-Pour Point Oil Field In Hungary. (2022).
22. Hakiki F., and Wibowo, A.T.. Formulation of Rock Type Prediction in Cored Well Using Fuzzy Substractive Clustering Algorithm, Proceeding Indonesian Petroleum Association 38th Annual Convention and Exhibition, IPA14-SE-118. (2014).
23. E. Ebeltoft, F. Lomeland, A. Brautaset, Å. Haugen, Parameter Based SCAL – Analysing Relative Permeability for Full Field Application. In International Symposium of the Society of Core Analysts, Avignon, France, (2014).
24. F. Lomeland, E. Ebeltoft, W. H. Thomas, A New Versatile Relative Permeability Correlation. In International Symposium of the Society of Core Analysts, Toronto, Canada, (2005).
25. Wibowo, A. S., Permadi, P., A type curve for carbonates rock typing. Presented at the International Petroleum Technology Conference, Beijing, 26-28 March. IPTC-16663-MS. https://doi.org/10.2523/IPTC-16663-MS, (2013).
26. Kozeny, J., Über Kapillare Leitung des Wassers im Boden. Sitzungsber. Akad.Wiss. Wien 136:271–306, (1927).
27. Wibowo, A. S., Carbonate Characterization Based on Pore Geometry And Structure, PhD Dissertation, Bandung Institute of Technology, (2014).
28. M. Junita & Permadi, Pudji & Widarsono, Bambang., *Connecting Microscopic Geological Features to Pore Geometry and Pore Structure: Case Study - Sandstone Reservoir of Balikpapan Formation, Kutai Basin*. Journal of Modern Applied Science. 12(1):51, (2017).
29. Palabiran, M., Sesilia, N., & Akbar, M. N. A., An Analysis of Rock Typing Methods in Carbonate Rocks For Better Carbonate Reservoir Characterization: A Case Study of Minahaki Carbonate Formation, Banggai Sula Basin, Central Sulawesi, (2016).
30. M.N.A. Akbar, and R. Myhr., *Dynamic Reservoir Rock Typing for Supercritical CO2-Brine System in Sandstone*. In SPE *Norway Subsurface Conference,* Bergen, Norway, (2024).
31. Lomeland, F., et al., A Versatile Representation of Upscaled Relative Permeability for Field Applications, SPE154487, SPE Europec/EAGE Annual Conference, 4-7 June, Copenhagen, Denmark, (2012).
32. Spiteri, E.J., et al., A New Model of Trapping and Relative Permeability Hysteresis for All Wettability Characteristics. SPE Journal, Vol. 13 03 p.277-288, (2008).
33. Craig Jr., F.F., The Reservoir Engineering Aspects of Waterflooding. SPE Monograph Series. Vol. 3. Society of Petroleum Engineers. (1993).
34. Anderson, W.G., Wettability Literature Survey Part 5: The Effects of Wettability on Relative Permeability. Journal of Petroleum Technology, 39(11): p. 1453-1468, (1987).
35. Buckley, J.S., K. Takamura, and N.R. Morrow, Influence of Electrical Surface Charges on the Wetting Properties of Crude Oils. 1989. SPERE, Vol.4 03, p. 332-340, (1989).
36. Buckley, J.S., C. Bousseau, and Y. Liu, Wetting Alteration by Brine and Crude Oil: From Contact Angles to Cores,. SPEJ Vol.1 03 p.341-350, (1996).
37. Yu, L. and J.S. Buckley, Evolution of Wetting Alteration by Adsorption From Crude Oil. SPE Formation Evaluation, Vol.12 01, p. 5-12 (1997).

38. Buckley, J.S. and Y. Liu, Some mechanisms of crude oil/brine/solid interactions. Journal of Petroleum Science and Engineering, 20(3–4): p. 155-160. (1998).
39. Buckley, J.S., Y. Liu, and S. Monsterleet, Mechanisms of Wetting Alteration by Crude Oils. SPEJ, Vol. 3 01 p.54-61, (1998).
40. Loahardjo, N., et al., Oil Recovery by Sequential Waterflooding: the Effects of Aging at Residual Oil and Initial Water Saturation, SPE154202, in SPE Improved Oil Recovery Symposium. Society of Petroleum Engineers: Tulsa, Oklahoma, USA. (2012).

Appendix

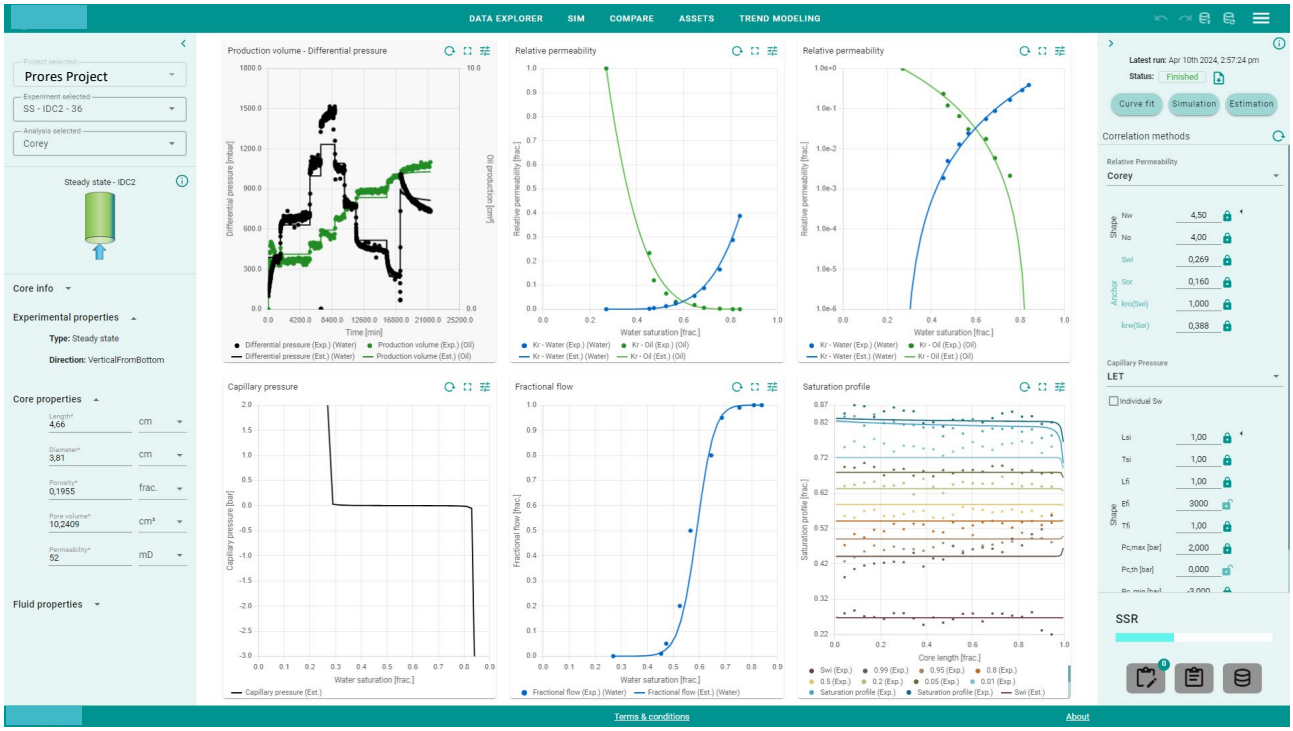

Fig. A-1. Production forecast profile in oil discovery X displaying the uncertainty span derived from the new Corey trend modelling method.

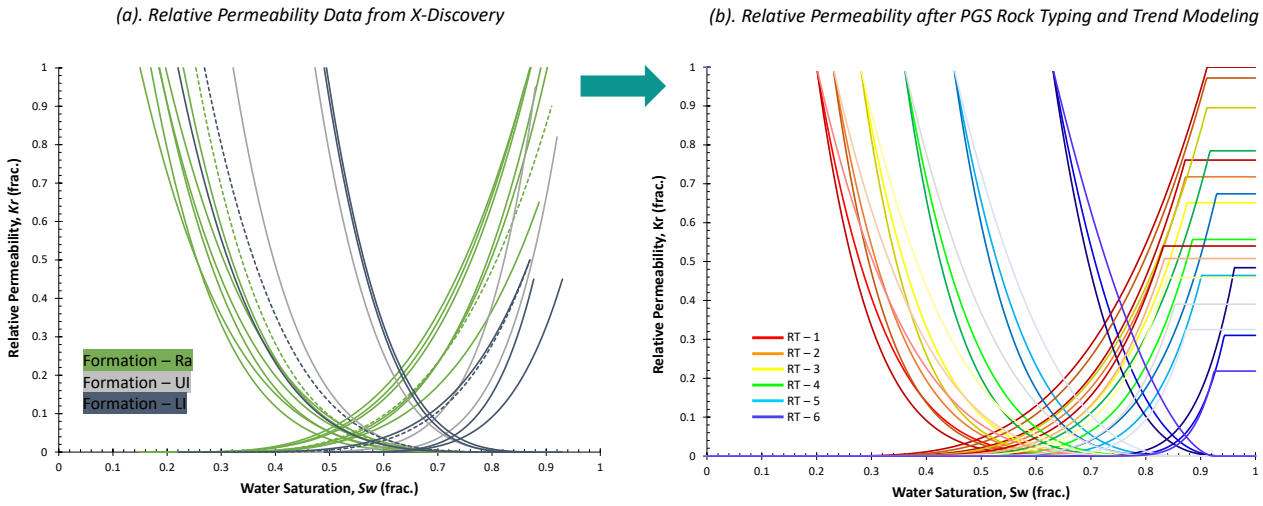

Fig. A-2. Comparison for relative permeability curves between the experimental relative permeability curves (left) and relative permeability curves generated using Corey trend modelling with PGS rock typing (right).